Bioelectrochemistry xxx (2015) xxx–xxx

Contents lists available at ScienceDirect

Bioelectrochemistry

journal homepage: www.elsevier.com/locate/bioelechem

The effect of temperature on electrochemically driven denaturation monitored by SERS

Evanthia Papadopoulou [a], Marta Meneghello [a], Pietro Marafini [b], Robert P. Johnson [a], Tom Brown [b], Philip N. Bartlett [a,*]

[a] Chemistry, University of Southampton, Highfield, Southampton SO17 1BJ, UK
[b] Department of Chemistry, University of Oxford, Chemistry Research Laboratory, Oxford OX1 3TA, UK

ARTICLE INFO

Article history:
Received 23 October 2014
Received in revised form 11 May 2015
Accepted 21 June 2015
Available online xxxx

Keywords:
DNA stability
SERS
Biosensor
Temperature
Electrochemically driven melting
E-melting

ABSTRACT

Scanning the electrochemical potential negative results in the gradual denaturation of dsDNA immobilised at a nanostructure gold electrode, the DNA melting is monitored by SERS. We demonstrate the effect of the experimental temperature on the electrochemically driven melting (*E*-melting) by carrying out experiments between 10 and 28 °C using two DNA duplexes (20 and 21 base pairs). Significant temperature dependence for both the melting potentials, E_m, and the steepness of the melting curves was found over the range 10 to 18 °C. Above 18 °C the results were found to be independent of temperature. The relative temperature insensitivity of the melting potentials above 18 °C is advantageous for the application of the electrochemically driven melting technique because precise temperature control is not necessary for measurements that are carried out around room temperature. Conversely temperature dependence below 18 °C offers a way to improve discrimination for highly similar DNA sequences.

© 2015 Elsevier B.V. All rights reserved.

1. Introduction

Detection and identification of specific DNA sequences are critical in clinical diagnostics [1], drug screening [2] and forensic analysis [3]. Optical and electrochemical DNA-biosensors have attracted particular attention due to their sensitivity, robustness, low cost and ability to carry out multi-target analysis. Both types of DNA biosensors rely for their specificity on DNA hybridization. The most common optical biosensors usually utilise techniques such as fluorescence [4–6], fluorescence resonance energy transfer (FRET) [7,8] or surface Plasmon resonance (SPR) [9,10]. Fluorescence based techniques measure the emission intensity of a dye-labelled probe DNA or an intercalating dye after hybridization whereas surface plasmon resonance methods utilise the change in the refractive index at the SPR sensor surface upon hybridization with a surface bound probe. On the other hand, electrochemical biosensors use electrical measurement and can be based either on changes in impedance [11,12] or on the measurement of redox currents [13].

Surface-enhanced Raman spectroscopy (SERS) is an alternative technique that has attracted interest in the development of DNA sensors due to the high sensitivity of the technique and the specificity provided by the use of vibrational spectroscopy. Label free approaches that directly detect the distinctive SERS spectra from DNA bases have been reported [14–17], in particular the discrimination of single base-mismatches within short single stranded oligonucleotides has been shown [14]. Although these approaches do not require a hybridization event to discriminate DNA sequences, they have currently been restricted to studies of short (<25 base pairs (bp)) synthetic DNA samples and no data have been published that show discrimination of long (>100 bp) DNA strands generated from biological samples. Attaching Raman dye-labelled oligonucleotides to SERS substrates [18–20] or utilising dye-coded nanoparticles [21,22] generates strong, specific Raman signals, permitting identification of a large number of oligonucleotides without the need for separation. These techniques have been demonstrated to be useful for the analysis of clinical samples. However they are usually hybridization-based, thus they are not sensitive enough to very small differences in the DNA such as single base mutations.

Alternatively, DNA discrimination can be achieved using techniques that exploit the denaturation of DNA rather than the hybridization. The most popular examples are real-time polymerase chain reaction (PCR) in conjunction with absorption/fluorescence melting analysis [23] and denaturating gradient gel electrophoresis that uses a gel to separate DNA fragments according to their melting characteristics (DGGE) [24,25]. Both techniques require expensive instrumentation. Electrochemical techniques can also be used to monitor the denaturation. This "electrochemical melting" [26,27] is distinct from the process described here as the melting of the dsDNA is brought about thermally but detected electrochemically. Thus, for example in early work in this area

Abbreviations: bp, base pair; *E*-melting, electrochemically driven melting.

* Corresponding author.
E-mail address: P.N.Bartlett@soton.ac.uk (P.N. Bartlett).

http://dx.doi.org/10.1016/j.bioelechem.2015.06.007
1567-5394/© 2015 Elsevier B.V. All rights reserved.

Please cite this article as: E. Papadopoulou, et al., The effect of temperature on electrochemically driven denaturation monitored by SERS, Bioelectrochemistry (2015), http://dx.doi.org/10.1016/j.bioelechem.2015.06.007

Paleček used polarography to study conformational changes in DNA with temperature [28]. More recently techniques such as cyclic voltammetry [29], square wave voltammetry [30], differential pulse voltammetry [26,27,31] and AC voltammetry [32] have all been used to monitor the thermally driven melting of dsDNA at electrode surfaces. In contrast we have developed an alternative denaturation-based approach to discriminate DNA sequences in which we use electrochemically driven denaturation (*E*-melting) of double-stranded (ds) DNA immobilised at a nanostructured gold electrode where the DNA melting is monitored by SERS. Electrochemically driven melting has been reported by several authors. Early studies by Brabec and Palecek observed melting of dsDNA adsorbed on mercury electrodes [33], and Sosnowski et al. [34] described electrochemically driven denaturation of dsDNA bound to an agarose gel up to 1 μm above a Pt electrode surface. In addition, Hassmann et al. [35,36] described studies in which they covalently attached nucleic acid probes to conducting polycarbonate/carbon fibre electrodes and showed that complementary oligonucleotides were enriched at the electrodes by cyclic inversion of an electrochemical potential between −0.2 and −1.5 V vs. Ag/AgCl. In our work a DNA target labelled with a fluorophore is hybridised to a surface bound probe, followed by the application of a suitably negative potential so that the dsDNA melts [37]. *E*-melting curves, constructed by plotting the SERS intensity of the fluorophore Raman signal against the electrode potential, are then used to discriminate DNA sequences based on differences in the stability of the dsDNA [38]. This technique relies on the fact that the less stable DNA duplexes e.g. duplexes containing a single base mutation, will have less negative denaturation (melting) potentials. Sphere segment void (SSV) Au surfaces [39] are used as the SERS substrates due to their large and reproducible SERS enhancements, well defined surface areas and good electrochemical stability [40–43].

We have demonstrated that this methodology is sensitive, robust and suitable for analysis of DNA generated from biological samples. More precisely, we showed discrimination of genetic markers and pathogenic bacteria by targeting short tandem repeats [44] and single nucleotide polymorphism [37,38,45] with detection limits of 0.3 μM without the need for prior-purification of the DNA samples. In addition, electrochemical potentials were found to be insensitive to changes in the local pH over the range 6–8 [46]. Most significantly, we have recently demonstrated the discrimination of nucleotide polymorphism in long (>250 bp) PCR amplicons which allowed us to distinguish DNA generated from *Yersinia pestis*, the causative agent of plague, from the closely related species *Y. pseudotuberculosis* [45]. In this case the discrimination was significantly improved when the experiments were conducted at lower temperature due to the slope of the wild type amplicon melting profile being steeper when compared to that recorded at room temperature.

In the current study we expand this work to examine in greater detail the effect of the experimental temperature on the electrochemical melting potential and the sharpness of the melting curves. *E*-melting experiments were carried out for two different DNA duplexes, 20 and 21 bp, over a temperature range from 10 °C to 28 °C. The results clearly show a shift in the melting potential to more negative values coupled with sharper melting curves when the temperature is ≤18 °C. The results are of interest since *E*-melting experiments can be combined with reduced temperature to directly address more complicated problems for real life applications.

2. Material and methods

All reagents used were of analytical grade and obtained from Sigma-Aldrich unless otherwise stated. Oligonucleotide synthesis was performed using standard methods by ATDBio Southampton, United Kingdom. The DNA probes (Table 1) had a three di-thiol linker at the 5′ end (Fig. S1). The DNA target sequences were fully complementary to the probes and labelled with Texas Red.

Table 1
Oligonucleotide sequences used (5′–3′)[a].

DNA-2	XXXH-ATATCATCTTTGGTGTTTCCT
DNA-1	XXXH-AGGAAACACCAAAGATGATATT

[a] H = hexaethyleneglycol spacer; X = dithiol monomer.

2.1. Preparation of sphere segment void (SSV) substrates

A gold-chrome coated microscope slide was prepared by thermal vapour deposition of a 10 nm chromium adhesion layer followed by approximately 200 nm of gold onto a standard glass microscope slide. A monolayer template of 600 nm polystyrene spheres (Fisher Scientific, 1% wt. aqueous suspension) was formed at the surface using a convective assembly method. Gold was deposited through the template to a height of 480 nm at −0.72 V vs. SCE from commercial gold plating solution (ECF 60, Metalor) containing 100 μl brightener (E3, Metalor) in 20 ml of plating solution. After deposition the polystyrene spheres were removed by immersion in DMF (HPLC grade, Rathburn) for 30 min, and the substrates were rinsed in deionised water immediately before use.

2.2. Immobilisation of probe oligonucleotides on the substrate and DNA hybridization

The SSV substrates were incubated in a solution of 1 μM probe diluted in 10 mM Tris buffer (pH 7.2) containing 1 M NaCl overnight, at room temperature. After rinsing the substrates several times with 10 mM Tris buffer/1 M NaCl solution, the remaining surface was passivated by immersing the substrates in 10 mM mercaptohexanol diluted in 10 mM Tris/1 M NaCl buffer for 20 min. After passivation the substrates were rinsed with 10 mM Tris buffer/1 M NaCl solution. Hybridization of the surface bound probes to the labelled DNA targets was achieved by heating the substrates in 3 μM solutions of the targets diluted in 10 mM Tris buffer/1 M NaCl to 90 °C and then allowing it to cool slowly to room temperature in a water bath. The substrates were rinsed several times with 10 mM phosphate buffer/0.1 M NaCl (pH 7.2) and kept in the same buffer until used.

2.3. E-melting procedure

Electrochemically driven melting experiments were carried out in a custom-built thermostatically jacketed spectro-electrochemical Raman cell (Ventacon Ltd.), where the substrate is used as the working electrode, a platinum wire as the counter electrode, and silver/silver chloride pellet as the reference electrode. In a typical *E*-melting experiment, the potential was swept at 1 mV s^{-1} from a starting potential of −0.4 to −1.3 V in 10 mM phosphate buffer/0.1 M NaCl (pH 7.2). All electrochemical measurements were carried out using an EcoChemie AutolabIII potentiostat/galvanostat.

2.4. Raman instrumentation

Raman spectra were acquired using a 50× objective on a Renishaw 2000 microscope instrument equipped with a 632.8 nm He–Ne laser. The laser power was 2.3 mW and spectra were recorded with an exposure time of 5–15 s. The temperature was controlled by flowing water through the cell jacket via a computer controlled water bath (Grant, accuracy ±1 °C). The stability of the temperature during the measurement was monitored by a thermocouple built into the body of the cell. The actual temperature at the SSV surface was measured before the start of each experiment by a second thermocouple placed in contact with a cover slip in direct contact with the SSV surface.

Please cite this article as: E. Papadopoulou, et al., The effect of temperature on electrochemically driven denaturation monitored by SERS, Bioelectrochemistry (2015), http://dx.doi.org/10.1016/j.bioelechem.2015.06.007

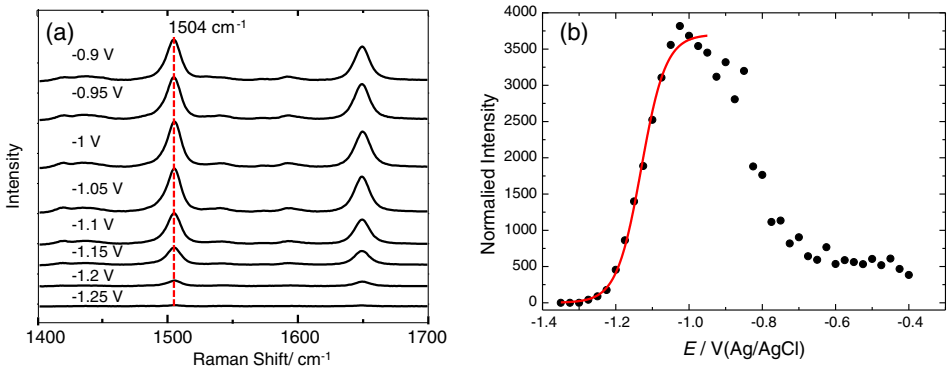

Fig. 1. (a) SERS spectra, acquired with 633 nm excitation laser, at increasingly cathodic potentials from the Texas Red labelled DNA target hybridised on DNA-1 probe vs. Ag/AgCl reference electrode at 10 °C. The spectra have been background subtracted and are all displayed with the same intensity scale but have been offset for clarity and normalised with respect to laser power and accumulation time. The potential was swept at a scan rate of 1 mV s^{-1} in 10 mM phosphate buffer (pH 7.2) containing 0.1 M NaCl. (b) Plot of the changes in the absolute signal intensities of the band at 1504 cm^{-1} as a function of applied potential. The red line shows the fitted *E*-melting curve from Eq. (1). (For interpretation of the references to colour in this figure legend, the reader is referred to the web version of this article.)

2.5. Data analysis

SERS spectra were baseline-corrected using a polynomial multipoint fitting function in Origin 9.1. The Raman intensities of the peaks are taken as height above the baseline. Origin 9.1 was used to fit sigmoidal curves to the melting profiles.

3. Results

3.1. DNA preparation and design

To study the effect of the experimental temperature on the *E*-melting, two different 21 and 22-bp double stranded DNA (dsDNA) sequences were used. The two sequences possess similar thermodynamic stabilities which can be seen from their calculated melting temperatures: 56.6 °C for DNA-1 and 57.2 °C for DNA-2 (both calculated using IDT OligoAnalyzer [47]). Similar conditions to the Raman experiments were used to calculate the melting temperatures (10 mM phosphate buffer, 0.1 M NaCl). The probe sequences for each duplex were immobilised on the Au SSV surface through three di-thiol linkers (5′-end) to ensure that they are strongly bound to the Au surface. The use of the three di-thiol linkers is important in order to ensure that the probe remains attached to the gold surface at high negative potentials required for the electrochemically driven melting as demonstrated in our earlier work [37]. The probes were subsequently hybridised with the target sequences, labelled with Texas Red, that were perfectly complementary to each probe. Texas Red is in resonance with the 633 nm excitation wavelength used in these experiments.

E-melting experiments for each sequence were performed at controlled temperatures in the range from 10 to 28 °C. The temperature was controlled by flowing water through the cell jacket via a computer controlled water bath (Grant, accuracy ± 1 °C). The temperature discrepancy between the water bath and the substrate surface was monitored by a thermocouple attached on the surface of the cell. In each experiment, the potential was ramped from a starting potential of −0.4 V to a final potential of −1.3 V vs. Ag/AgCl. Upon application of the negative potential the spectral intensities of the Texas Red bands at 1647 cm^{-1} (aromatic ring stretching) and 1504 cm^{-1} (N–H deformation) initially increased and then decreased sharply as the dsDNA on the surface started to denature. The initial increase in intensity is reversible and has been previously attributed to a change in orientation of the label with respect to the SSV surface [37]. Fig. 1 shows a typical set of SERS spectra of Texas Red as a function of the applied potential along with a plot of the intensity of the 1504 cm^{-1} Texas Red band as a function of potential.

3.2. The effect of temperature on E-melting

Fig. 2 shows the *E*-melting profiles of the two sequences at various temperatures. For each experiment, different SSV substrates were used and the spectra were acquired at different positions on the same substrate as the surface potential changes. The following sigmoidal fitting function was used to construct the melting curves

$$I = I_{max} - \frac{I_{max}}{(1 + \exp\left(\frac{E - E_m}{dE}\right)} \quad (1)$$

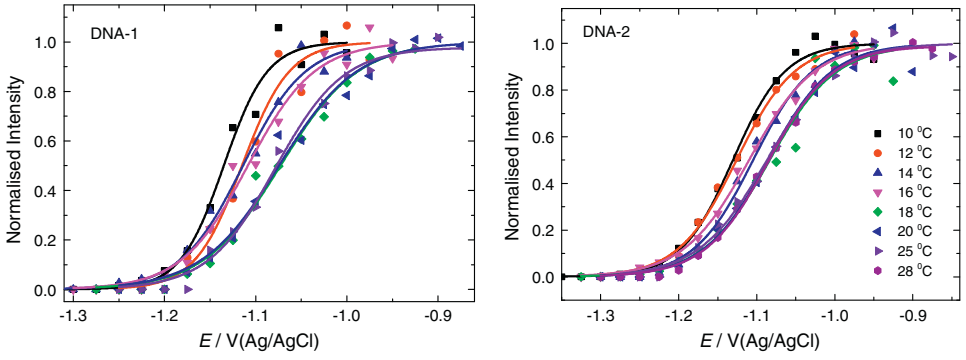

Fig. 2. *E*-melting curves of DNA-1 and DNA-2 at various temperatures (■ 10, ● 12, ▲ 14, ▼ 16, ♦ 18, ◄ 20, ► 25, and ✹ 28 °C). The potential was swept at a scan rate of 1 mV s^{-1} in 10 mM phosphate buffer (pH 7.2) containing 0.1 M NaCl.

Please cite this article as: E. Papadopoulou, et al., The effect of temperature on electrochemically driven denaturation monitored by SERS, Bioelectrochemistry (2015), http://dx.doi.org/10.1016/j.bioelechem.2015.06.007

Table 2
Experimental melting potentials (E_m) versus Ag/AgCl and dE values for dsDNA-1 and dsDNA-2 determined from the fitting of the data collected for each DNA to Eq. (1). E_m values versus NHE after conversion of the experimental values.

Experimental temperature/°C	E_m (expt.) vs. Ag/AgCl/mV	E_m vs. NHE/mV	dE/mV
DNA-1			
10	−1135 ± 5	−854 ± 5	24 ± 4
11	−1115 ± 6	−834 ± 6	26 ± 5
12	−1114 ± 6	−832 ± 6	34 ± 4
14	−1109 ± 6	−826 ± 6	37 ± 4
18	−1073 ± 6	−789 ± 6	42 ± 4
23	−1074 ± 6	−787 ± 6	43 ± 4
28	−1076 ± 5	−787 ± 5	39 ± 4
DNA-2			
10	−1131 ± 3	−850 ± 3	33 ± 3
12	−1126 ± 4	−844 ± 4	32 ± 3
14	−1105 ± 5	−822 ± 5	38 ± 4
16	−1098 ± 5	−814 ± 5	42 ± 3
18	−1084 ± 9	−800 ± 1	41 ± 7
20	−1086 ± 5	−801 ± 5	41 ± 4
25	−1087 ± 4	−799 ± 4	44 ± 3
28	−1085 ± 2	−796 ± 2	41 ± 2

where I is the absolute spectral intensity of the band at 1504 cm^{-1} at the applied potential E, I_{max} is the average intensity value at the plateau for the sigmoidal curve, E_m, is the melting potential when I equals $I_{max}/2$, and dE is a constant that describes the sharpness of the melting curve (the gradient of the curve at E_m is $I_{max}/4dE$). The data from each experiment were normalised to their respective I_{max} values before plotting the melting curves to allow direct comparison.

The reference electrode used in these experiments was a silver/silver chloride electrode immersed in the same solution as the working electrode (0.1 M NaCl). To directly compare the melting potentials at different temperatures the experimental values have been converted into potentials versus standard hydrogen electrode (NHE) at 25 °C. This conversion has been done using the Nernst equation, taking into account that the standard potential E^0 of Ag/AgCl against NHE (0.2222 V) and the activity coefficient for the 0.1 M NaCl solution (0.78) [48]. The effect of temperature on the potential of the Ag/AgCl electrode has been taken into account in this calculation (the temperature coefficient for the Ag/AgCl electrode in 0.1 M NaCl is 0.442 mV/deg) [48].

Table 2 shows the experimental melting potentials versus Ag/AgCl, calculated after each set of data was fitted to Eq. (1), and the temperature independent values versus NHE at different temperatures for DNA-1 and DNA-2. The overall change in the melting potential as a function of temperature, with the associated experimental errors calculated from the fitting, is shown in Fig. 3(a). The corresponding dE values that indicate the sharpness of the melting transitions, together with the associated experimental errors, are plotted as a function of temperature in Fig. 3(b). It is clear that for both DNA sequences that the melting potential shifts to less negative values as the experimental temperature increases up to 18 °C and thereafter reaches a plateau over the temperature range 18 to 28 °C. The dE values for both sequences show the same trend with an increase in dE, corresponding to less steep melting curves, up to ~18 °C and then a plateau thereafter. These results are consistent with increased thermodynamic stability of the dsDNA as the temperature decreases from 18 to 10 °C making it more difficult to electrochemically melt the DNA (a more negative potential is required). The corresponding increase in the sharpness in the melting transition suggests that the DNA melts more cooperatively approaching a two state transition from duplex to single strands at temperatures ≤18 °C.

4. Discussion

Early studies on the melting of short oligonucleotides using NMR showed that the terminal base pairs are unstable due to the tendency of the inter-base hydrogen bonds at the ends of the duplex to exchange with H-bonds to water (the solvent) [49–51]. Thus the terminal base pairs can break before those located inside the duplex. This effect is referred to as terminal end-fraying and leads to melting of DNA through a non-cooperative mechanism (the transition from duplex to single strands involves intermediate states). This thermal end-fraying is significant even at room temperature and reduces as the temperature decreases. Here, the temperature dependence of the E_m values for both of the DNA sequences suggest that the effect of end-fraying is progressively reduced at temperatures below 18 °C. As the temperature decreases, the DNA unwinding is mainly driven by electrochemical forces rather than a combination of electrochemical and thermal forces and the decrease in end-fraying allows the DNA to melt in a more cooperative manner, hence the sharper melting curves recorded at low temperatures along with more negative E_m values. Above 18 °C and up to 28 °C we see no significant effect of the experimental temperature on E_m or dE in our experiments. It is not clear why this should be. However being able to control the temperature along with the electrochemical potential is a significant advantage of the E-melting technique since by going to lower temperatures it is possible to significantly improve the sharpness of the melting transitions as well as the stability of the DNA duplexes and this can be used to improve the discrimination of closely similar DNA sequences. For example, we have recently shown that the detection of single nucleotide polymorphism within long PCR amplicons (≥250 bp) extracted from pathogenic bacteria and hybridised on 22 bases long surface bound probes, can be considerably improved if the experiments are carried out at 10 °C [45]. On the other hand the relative insensitivity of the E_m values above 18 °C can be advantageous because it means that very precise temperature control around room temperature (25 °C) is not necessary for most E-melting

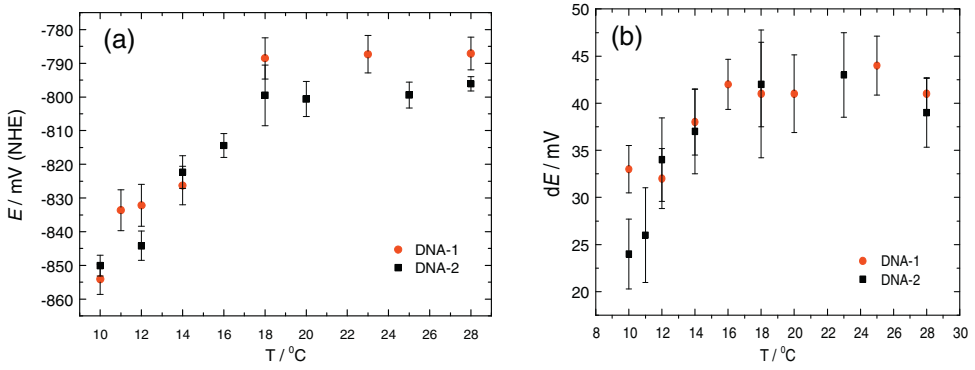

Fig. 3. (a) Melting potentials of dsDNA-1 and dsDNA-2 versus NHE plotted against the experimental temperature. (b) dE values of dsDNA-1 and dsDNA-2 against the experimental temperature. The experimental errors are calculated from the fitting.

Please cite this article as: E. Papadopoulou, et al., The effect of temperature on electrochemically driven denaturation monitored by SERS, Bioelectrochemistry (2015), http://dx.doi.org/10.1016/j.bioelechem.2015.06.007

ARTICLE IN PRESS

measurements. This is important and demonstrates the potential applicability of the technique as a clinical diagnostic tool.

5. Conclusions

E-melting experiments for two different short DNA duplexes (20 and 21 bp) possessing similar melting temperatures were carried out between 10 and 28 °C. A significant temperature dependence for both the melting potentials, E_m, and the steepness of the melting curves, described by d*E*, was found over the range 10 to 18 °C. The results are consistent with greater stability of the dsDNA at the lower temperature together with greater cooperativity in the melting, approaching a two state transition from duplex to single strands. These effects were reproducible for the two DNA sequences and can be attributed to the reduction of the thermal end-fraying as the experimental temperature drops to values < 18 °C. Both the electrochemical melting and sharpness of the melting transitions were found to be temperature independent in the region 18 to 28 °C.

The relative temperature insensitivity of the melting potentials above 18 °C is advantageous for the technique since it means that for most discriminations carried out at room temperature precise temperature control is not necessary. On the other hand the possibility to improve the dsDNA stability and increase the sharpness of the melting transition by moving to lower experimental temperatures can be useful to allow the *E*-melting technique to be used in the discrimination of highly similar DNA sequences.

Acknowledgements

E.P. acknowledges the Defence Science and Technology Laboratory (contract number DSTLX 1000061240) for funding this research. We thank Y-C. Lin for help with preliminary *E*-melting experiments. PNB gratefully acknowledges receipt of a Wolfson Research Merit award.

References

[1] P.W. Whitby, K.B. Carter, J.L. Burns, J.A. Royall, J.J. LiPuma, T.L. Stull, Identification and detection of *Stenotrophomonas maltophilia* by rRNA-directed PCR, J. Clin. Microbiol. 38 (2000) 4305–4309.
[2] F. Chen, Y.X. Zhao, Methylation-blocked enzymatic recycling amplification for highly sensitive fluorescence sensing of DNA methyltransferase activity, Analyst 138 (2013) 284–289.
[3] A.M. Divne, M. Allen, A DNA microarray system for forensic SNP analysis, Forensic Sci. Int. 154 (2005) 111–121.
[4] D.J. French, C.L. Archard, T. Brown, D.G. McDowell, HyBeacon (TM) probes: a new tool for DNA sequence detection and allele discrimination, Mol. Cell. Probes 15 (2001) 363–374.
[5] R.L. Stoermer, K.B. Cederquist, S.K. McFarland, M.Y. Sha, S.G. Penn, C.D. Keating, Coupling molecular beacons to barcoded metal nanowires for multiplexed, sealed chamber DNA bioassays, J. Amer. Chem. Soc. 128 (2006) 16892–16903.
[6] Y.G. Li, Y.T.H. Cu, D. Luo, Multiplexed detection of pathogen DNA with DNA-based fluorescence nanobarcodes, Nat. Biotechnol. 23 (2005) 885–889.
[7] F. Gao, P. Cui, X.X. Chen, Q.Q. Ye, M.G. Li, L. Wang, A DNA hybridization detection based on fluorescence resonance energy transfer between dye-doped core–shell silica nanoparticles and gold nanoparticles, Analyst 136 (2011) 3973–3980.
[8] T. Qiu, B. Zhang, Z.-Y. Hu, J.-H. Tang, H.-P. Xie, B.-R. Gu, Detection of DNA based on fluorescence resonance energy transfer of polyelectrolyte-protected CdTe quantum dots as energy donors, Analyst 137 (2012) 2608–2613.
[9] H. Sipova, J. Homola, Surface plasmon resonance sensing of nucleic acids: a review, Anal. Chim. Acta 773 (2013) 9–23.
[10] B.P. Nelson, T.E. Grimsrud, M.R. Liles, R.M. Goodman, R.M. Corn, Surface plasmon resonance imaging measurements of DNA and RNA hybridization adsorption onto DNA microarrays, Anal. Chem. 73 (2001) 1–7.
[11] S. Basuray, S. Senapati, A. Aijian, A.R. Mahon, H.-C. Chang, Shear and AC field enhanced carbon nanotube impedance assay for rapid, sensitive, and mismatch-discriminating DNA hybridization, ACS Nano 3 (2009) 1823–1830.
[12] S. Gruetzke, S. Abdali, W. Schuhmann, M. Gebala, Detection of DNA hybridization using electrochemical impedance spectroscopy and surface enhanced Raman scattering, Electrochem. Commun. 19 (2012) 59–62.
[13] E. Palecek, M. Masarik, R. Kizek, D. Kuhlmeier, J. Hassmann, J. Schulein, Sensitive electrochemical determination of unlabeled MutS protein and detection of point mutations in DNA, Anal. Chem. 76 (2004) 5930–5936.
[14] E. Papadopoulou, S.E.J. Bell, Label-free detection of single-base mismatches in DNA by surface-enhanced Raman spectroscopy, Angew. Chem. Int. Ed. 50 (2011) 9058–9061.
[15] E. Papadopoulou, S.E.J. Bell, Label-free detection of nanomolar unmodified single- and double-stranded DNA by using surface-enhanced Raman spectroscopy on Ag and Au colloids, Chem. Eur. J. 18 (2012) 5394–5400.
[16] A. Barhoumi, D. Zhang, F. Tam, N.J. Halas, Surface-enhanced Raman spectroscopy of DNA, J. Amer. Chem. Soc. 130 (2008) 5523–5529.
[17] V.V. Thacker, L.O. Herrmann, D.O. Sigle, T. Zhang, T. Liedl, J.J. Baumberg, U.F. Keyser, DNA origami based assembly of gold nanoparticle dimers for surface-enhanced Raman scattering, Nat. Commun., 5 (2014) 3448–3448.
[18] K. Gracie, E. Correa, S. Mabbott, J.A. Dougan, D. Graham, R. Goodacre, K. Faulds, Simultaneous detection and quantification of three bacterial meningitis pathogens by SERS, Chem. Sci. 5 (2014) 1030–1040.
[19] T. Vo-Dinh, K. Houck, D.L. Stokes, Surface-enhanced Raman gene probes, Anal. Chem. 66 (1994) 3379–3383.
[20] M.B. Wabuyele, T. Vo-Dinh, Detection of human immunodeficiency virus type 1 DNA sequence using plasmonics nanoprobes, Anal. Chem. 77 (2005) 7810–7815.
[21] D. Graham, D.G. Thompson, W.E. Smith, K. Faulds, Control of enhanced Raman scattering using a DNA-based assembly process of dye-coded nanoparticles, Nat. Nanotechnol. 3 (2008) 548–551.
[22] T. Kang, S.M. Yoo, I. Yoon, S.Y. Lee, B. Kim, Patterned multiplex pathogen DNA detection by Au particle-on-wire SERS sensor, Nano Lett. 10 (2010) 1189–1193.
[23] E.A. Tindall, D.C. Petersen, P. Woodbridge, K. Schipany, V.M. Hayes, Assessing high-resolution melt curve analysis for accurate detection of gene variants in complex DNA fragments, Hum. Mutat. 30 (2009) 876–883.
[24] R. Fodde, M. Losekoot, Mutation detection by denaturing gradient electrophoresis (DGGE), Hum. Mutat. 3 (1994) 83–94.
[25] L. Lodewyckx, C. Vandevyver, C. Vandervorst, W. Van Steenbergen, J. Raus, L. Michiels, Mutation detection in the alpha-1 antitrypsin gene (PI) using denaturing gradient gel electrophoresis, Hum. Mutat. 18 (2001) 243–250.
[26] H. Nasef, V. Beni, C.K. O'Sullivan, Electrochemical melting-curve analysis, Electrochem. Commun. 12 (2010) 1030–1033.
[27] H. Nasef, V. Beni, C.K. O'Sullivan, Labelless electrochemical melting curve analysis for rapid mutation detection, Anal. Methods 2 (2010) 1461–1466.
[28] E. Paleček, M. Bartošík, Electrochemistry of nucleic acids, Chem. Rev. 112 (2012) 3427–3481.
[29] Y. Mao, C. Luo, Q. Ouyang, Studies of temperature-dependent electronic transduction on DNA hairpin loop sensor, Nucleic Acids Res. 31 (2003) e108.
[30] Z. Zabost, A.M. Nowicka, M. Donten, Z. Stojek, Substantial difference between temperature dependencies of dsDNA predenaturation process obtained by voltammetry and spectroscopy, Phys. Chem. Chem. Phys. 11 (2009) 8933–8938.
[31] X. Luo, I.-M. Hsing, Real time electrochemical monitoring of DNA/PNA dissociation by melting curve analysis, Electroanalysis 21 (2009) 1557–1561.
[32] A.-E. Surkus, G.-U. Flechsig, Electrochemical detection of DNA melting curves by means of heated biosensors, Electroanalysis 21 (2009) 1119–1123.
[33] V. Brabec, E. Palecek, Interaction of nucleic-acids with electrically charged surfaces: II. Conformational-changes in double-helical polynucleotides, Biophys. Chem. 4 (1976) 79–92.
[34] R.G. Sosnowski, E. Tu, W.F. Butler, J.P. Oconnell, M.J. Heller, Rapid determination of single base mismatch mutations in DNA hybrids by direct electric field control, Proc. Natl. Acad. Sci. U. S. A. 94 (1997) 1119–1123.
[35] J. Hassmann, A. Misch, J. Schülein, J. Krause, B. Graßl, P. Müller, W.M. Bertling, Development of a molecular diagnosis assay based on electrohybridization at plastic electrodes and subsequent PCR, Biosens. Bioelectron. 16 (2001) 857–863.
[36] J. Schülein, B. Graßl, J. Krause, C. Schulze, C. Kugler, P. Müller, W.M. Bertling, J. Hassmann, Solid composite electrodes for DNA enrichment and detection, Talanta 56 (2002) 875–885.
[37] S. Mahajan, J. Richardson, T. Brown, P.N. Bartlett, SERS-melting: a new method for discriminating mutations in DNA sequences, J. Amer. Chem. Soc. 130 (2008) 15589–15601.
[38] R.P. Johnson, R. Gao, T. Brown, P.N. Bartlett, The effect of base-pair sequence on electrochemically driven denaturation, Bioelectrochem. 85 (2012) 7–13.
[39] P.N. Bartlett, J.J. Baumberg, P.R. Birkin, M.A. Ghanem, M.C. Netti, Highly ordered macroporous gold and platinum films formed by electrochemical deposition through templates assembled from submicron diameter monodisperse polystyrene spheres, Chem. Mater. 14 (2002) 2199–2208.
[40] S. Mahajan, J.J. Baumberg, A.E. Russell, P.N. Bartlett, Reproducible SERRS from structured gold surfaces, Phys. Chem. Chem. Phys. 9 (2007) 6016–6020.
[41] S. Cintra, M.E. Abdelsalam, P.N. Bartlett, J.J. Baumberg, T.A. Kelf, Y. Sugawara, A.E. Russell, Sculpted substrates for SERS, Faraday Discuss. 132 (2006) 191–199.
[42] T.A. Kelf, Y. Sugawara, J.J. Baumberg, M. Abdelsalam, P.N. Bartlett, Plasmonic band gaps and trapped plasmons on nanostructured metal surfaces, Phys. Rev. Lett. 95 (2005).
[43] R.M. Cole, J.J. Baumberg, F.J. Garcia de Abajo, S. Mahajan, M. Abdelsalam, P.N. Bartlett, Understanding plasmons in nanoscale voids, Nano Lett. 7 (2007) 2094–2100.
[44] D.K. Corrigan, N. Gale, T. Brown, P.N. Bartlett, Analysis of short tandem repeats by using SERS monitoring and electrochemical melting, Angew. Chem. Int. Ed. 49 (2010) 5917–5920.
[45] E. Papadopoulou, S.A. Goodchild, D.W. Cleary, S. Weller, N. Gale, T. Brown, P.N. Bartlett, Detection of single nucleotide polymorphism in unpurified PCR amplicons of Yersinia pestis bacteria by SERS and electrochemical melting, Anal. Chem. 87 (2015) 1605–1612.
[46] R.P. Johnson, J.A. Richardson, T. Brown, P.N. Bartlett, Real-time surface-enhanced raman spectroscopy monitoring of surface pH during electrochemical melting of double-stranded DNA, Langmuir 28 (2012) 5464–5470.
[47] IDT, https://eu.idtdna.com/analyzer/Applications/OligoAnalyzer/) in.

Please cite this article as: E. Papadopoulou, et al., The effect of temperature on electrochemically driven denaturation monitored by SERS, Bioelectrochemistry (2015), http://dx.doi.org/10.1016/j.bioelechem.2015.06.007

ARTICLE IN PRESS

[48] A.J. de Bethune, T.S. Licht, N. Swendeman, The temperature coefficients of electrode potentials. The isothermal and thermal coefficients — the standard ionic entropy of electrochemical transport of the hydrogen ion, J. Electrochem. Soc. 106 (1959) 616–625.
[49] D.J. Patel, Peptide antibiotic–oligonucleotide interactions — nuclear magnetic resonance investigations of complex formation between actinomycin-D and D-APTPGPCPAPT in aqueous solution, Biochem. 13 (1974) 2396–2402.
[50] S. Kundu, S. Mukherjee, D. Bhattacharyya, Effect of temperature on DNA double helix: an insight from molecular dynamics simulation, J. Biosci. 37 (2012) 445–455.
[51] D.J. Patel, S.A. Kozlowski, L.A. Marky, C. Broka, J.A. Rice, K. Itakura, K.J. Breslauer, Premelting and melting transitions in the D(CGCGAATTCGCG) self-complementary duplex in solution, Biochem. 21 (1982) 428–436.

Please cite this article as: E. Papadopoulou, et al., The effect of temperature on electrochemically driven denaturation monitored by SERS, Bioelectrochemistry (2015), http://dx.doi.org/10.1016/j.bioelechem.2015.06.007